Multiphase Ozonolysis of Organics in Wastewater by a Novel Membrane Reactor

Asim K. Guha, Purushottam V. Shanbhag, and Kamalesh K. Sirkar
Dept. of Chemical Engineering, Chemistry and Environmental Science, New Jersey Institute of Technology, University Heights, Newark, NJ 07102

David A. Vaccari
Dept. of Civil, Environmental and Coastal Engineering, Stevens Institute of Technology, Castle Point on the Hudson, Hoboken, NJ 07030

Deven H. Trivedi
Dept. of Chemistry and Chemical Engineering, Stevens Institute of Technology, Castle Point on the Hudson, Hoboken, NJ 07030

Conventional ozonation of recalcitrant organic compounds in wastewater suffers from low transfer rate of ozone into water. The low transfer rate can be enhanced by adding an inert fluorocarbon (FC) liquid immiscible with water but having a much higher solubility for ozone. A novel membrane reactor was studied for the destruction of organic pollutants by using FC liquid simultaneously as a reaction medium and a liquid membrane. The membrane reactor consisted of two sets of microporous and/or nonporous hollow-fiber membranes well-mixed in a cylindrical shell filled with the inert FC liquid. Wastewater was allowed to flow through the lumen of one set of microporous fibers; O_3-containing gas flowed through the bore of the other set. Oxidative degradation products get partitioned back into the two mobile phases. Degradation of such pollutants as phenol, acrylonitrile, nitrobenzene, trichloroethylene, and toluene in such a reactor is presented. The kinetics of degradation of each pollutant in the two-phase (aqueous – FC) system were studied using batch and semibatch experiments. Simulation results based on a first-order model to predict the behavior of pollutant degradation in such a membrane reactor are compared with experimental data.

Introduction

A number of processes and techniques employ oxidative degradation to treat high-strength wastewaters containing recalcitrant organic compounds. These include wet air oxidation (WAO), supercritical water oxidation (SCWO), direct ozonation, and advanced oxidation processes (AOP) like UV with H_2O_2 or UV with ozone. Liquid-phase processes in WAO employ high temperatures (150–350°C) and pressures (20–200 atm) as in the Zimpro process (Zimmerman, 1958). SCWO processes utilize much harsher reaction conditions to achieve an essentially complete conversion and mineralization (Modell et al., 1982). Although advanced oxidation processes like UV/H_2O_2, UV/O_3 are effective under ambient conditions, they can be quite costly (Sundstrom et al., 1989). The efficiency of single reactive oxidants O_3, H_2O_2 and so on is low both due to limitations of chemical kinetics as well as indiscriminate consumption of reactive free radicals by nontargeted contaminants in wastewater (Glaze and Kang, 1989). Low solubility of ozone in water and low O_3 concentration in the gaseous stream contribute significantly to this low efficiency.

We describe here a novel membrane reactor that addresses many such inefficiencies of ozonation. Consider first the low O_3 transfer rate in single-phase direct ozonation. One method of enhancing the mass-transfer rate in gas–liquid reaction involves adding a second liquid phase (may or may not be inert) immiscible with the first but in which the solute gas, for

Correspondence concerning this article should be addressed to K. K. Sirkar.
Present address of D. H. Trivedi: Foster Wheeler USA Corporation, Clinton, NJ 08801.

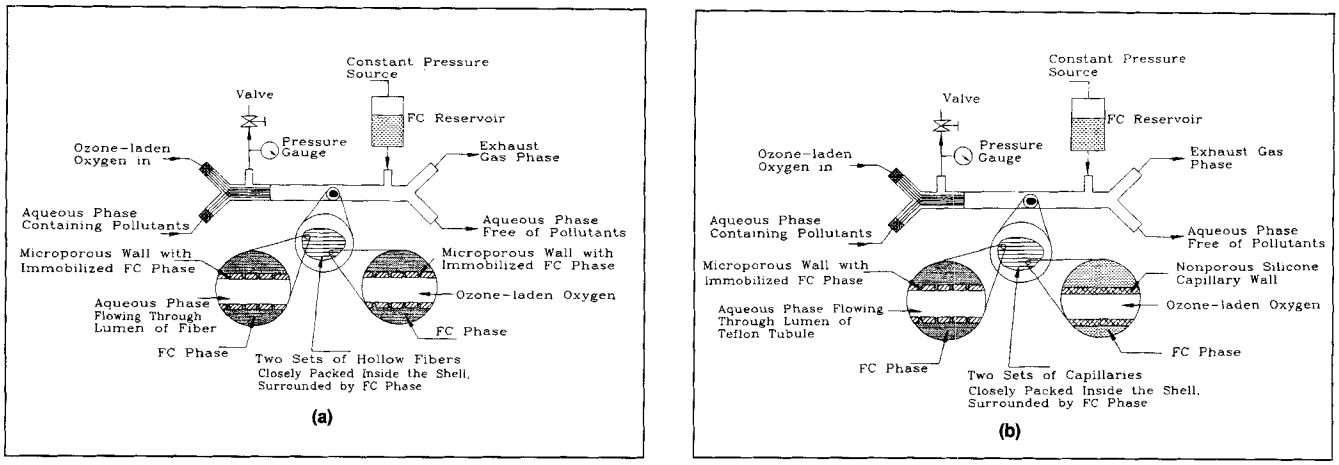

Figure 1. Membrane reactor comprising: (a) two sets of microporous hydrophobic hollow fibers; (b) microporous hydrophobic tubules or hollow fibers as one set and nonporous silicone capillaries as the other set.

example, O_3 is much more soluble. By adding an inert fluorocarbon (FC) solvent to wastewater in ozonation of phenol and β-naphthol, Stich and Bhattacharyya (1987) obtained a destruction rate almost an order of magnitude larger compared to direct aqueous-phase ozonation. This was attributed to 12 to 14 times higher O_3 solubility in fluorocarbon than in water. Such fluorocarbons are inert (often used as artificial blood), are essentially insoluble in water, and are not implicated in upper atmosphere O_3-destroying chemistry. Further, O_3-scavenging inorganic nontarget contaminants in water are absent from the FC phase.

Two-phase ozonation has another advantage. Organic pollutants in water having higher solubility in fluorocarbon will be present at much higher concentrations in FC resulting in higher reaction rates. This aspect is absent in Stich and Bhattacharyya (1987) since they studied phenol that has a very low solubility in FC. Further, Stich and Bhattacharyya (1987) required three devices, an O_3 saturator vessel for FC, a stirred two-phase aqueous-ozonated fluorocarbon reactor, and a two-phase separator. This process has many inefficiencies, such as reduction of FC loss by volatilization requires using FC having lower vapor pressure and high viscosity, leading to problems of dispersing the FC phase.

This dispersion-based multidevice process has been replaced by a single, compact, and nondispersive membrane reactor capable of achieving the intrinsically high efficiencies of FC-phase ozonolysis. In this membrane reactor, wastewater flows through the bore of one set of microporous hydrophobic hollow fibers (Figure 1a). Ozonated air flows through a second set of similar hollow fibers intimately mixed with the first set. The interstitial shell-side space between the two fibers sets contains the stationary FC liquid at a pressure lower than those of the other phases. The pores in both fibers are spontaneously wetted by the FC phase. The gas–FC liquid interface is immobilized at the inner surface of the second set of fibers (Sirkar, 1992); the FC-wastewater interface is immobilized similarly at the inner surface of the first fiber set. Pollutants from the wastewater flowing in the first fiber set are extracted nondispersively (Prasad and Sirkar, 1988) into the FC phase in the fiber pores and then into the shell-side FC film. They are oxidized immediately by O_3 supplied from the second fiber set into the FC film. Nonvolatile oxidative degradation products are back extracted into the aqueous effluent exiting the reactor through the first fiber set. Gaseous oxidation products are preferentially stripped out by the gas stream flowing in the second fiber set.

A slightly different tubular membrane reactor (Figure 1b) employs nonporous but highly O_3 permeable silicone rubber capillaries as the second set of fibers. This virtually eliminates the loss of FC vapor into the ozonated air stream; yet transfer rates of O_3 and O_2 through silicone rubber capillaries are not too much lower than those in direct gas–liquid contact.

These multimembrane two-phase ozonation reactors combine many functions. First, the two sets of hollow fiber membranes "contain" a reaction medium with a very high solubility for reactants. The first set of fibers allows concentration of one reactant (an act of separation) by solvent extraction and subsequent product removal by back extraction of degradation products. The second set of fibers facilitates simultaneously concentration of the second reactant (O_3) by absorption or membrane permeation and stripping of gaseous degradation products, for example, CO_2. Such multifunctional capabilities are novel for membrane reactors (Itoh and Govind, 1989; Kim and Datta, 1992; Chen et al., 1992) and potentially attractive for other separation-reaction-separation processes with or without catalysts. Both reactors can also be identified as a hollow fiber contained liquid membrane reactor (HFCLMR). The appropriate immobilized reaction medium also acts as a membrane, preventing nonreactants from contacting one another and controlling the rate at which the reactants can permeate given certain reaction rates. In fact, conditions must be such that the liquid membrane allows a high rate of reactants intake (O_3 and pollutants), but must prevent pollutants from going to the other side of the liquid film.

An evaluation of pollutant degradation in such a reactor requires knowledge of O_3 solubility in FC phase, partition coefficients of individual pollutants between water and FC phase, and pollutant degradation kinetics in such a two-phase system. The partition coefficient m_A of a species A is defined as

$$m_A = C_A^F / C_A^W \quad (1)$$

where C_A^F and C_A^W are equilibrium concentrations of species A in the fluorocarbon and the aqueous phases, respectively. The partition coefficient may be a strong function of the solubility of the pollutant in the FC phase and in water. Hydrophobic pollutants having a very low solubility in water may have a high solubility in the FC phase, thus providing a higher pollutant concentration to enhance the reaction rate.

Ozonation kinetics of pollutants in water are available (Langlais et al., 1991). Some information on kinetics of ozonation of different organic compounds in CCl_4 is also available (Pryor et al., 1983, 1984; Nakagawa et al., 1960). The presence of both organic and aqueous phases, however, requires independent kinetic studies due to the dynamics of reactants and products partitioning between the two phases. Kinetic studies should recognize here the possibility of two limiting conditions: pollutants having a low partition coefficient into the FC phase so that O_3 may be in excess, as opposed to the pollutants having a high partition coefficient where the amount of ozone available in the FC phase may become a limiting factor.

We illustrate here the oxidative degradation capability of a nondispersive fluorocarbon-based compact membrane reactor for efficient multiphase ozonolysis. The pollutants studied are: phenol, trichloroethylene (TCE), toluene, nitrobenzene, and acrylonitrile. They represent broad classes of toxic organic compounds encountered frequently in wastewaters. A model describing the reactor performance for degradation of a pollutant like phenol having a low solubility in the FC phase is also presented. The concurrent kinetic studies help to understand the phenomena of extraction and reaction at the two-phase interfaces and provide a basis for additional future studies.

Experimental Details

Experimental details and procedures are described here via the following categories: distribution coefficient of organic pollutants in FC/wastewater systems, solubility of ozone in FC phase, degradation kinetics of pollutants in a two-phase system, tubular membrane reactors, and the experimental setup to investigate membrane reactor performance.

Distribution coefficient of organic pollutants in FC/wastewater systems

The fluorocarbon solvents used were FC-43 and FC-77 (FLUORINERT, 3M, St. Paul, MN). Physical properties of these liquids are presented in Table 1. Pollutant distribution coefficient was determined at 25°C by mixing known volumes of FC phase and aqueous solution of the pollutant thoroughly for one hour followed by phase separation for half an hour. For pollutants with very low solubilities in water and high volatilities (toluene and TCE), a predetermined volume of pure pollutant was directly injected into a known volume of the water/FC-phase system. The aqueous phase was then sampled to determine the equilibrium concentration. The aqueous phase was analyzed for the pollutant using a high performance liquid chromatograph (HPLC). The HPLC (HP 1090A, Hewlett-Packard, Paramus, NJ) was equipped with a Micromeritics autosampler connected to a Valco valve having a 10-μL sample loop. A 10-cm-long and 3-mm-dia. Hypersil ODS glass column (Chrompack, Bridgewater, NJ) and a UV filter photometric detector were used. The amount of pollutant partitioning into the FC phase was determined by an overall mass balance (Trivedi, 1992; Shanbhag, 1992).

Ozone was generated by a Polymetrics (Colorado Springs, CO) ozone generator, using a pure O_2 cylinder (Extra Dry) (Matheson, E. Rutherford, NJ). The ozonator was operated at a voltage setting of 90 V, the pressure within the ozonator was kept at 163.4 kPa (9 psig), and the gas was passed through the ozonator at a constant flow rate of 0.6 std. L/min. A small portion of the ozonated gas was used for reaction; the major portion was vented after passing through two potassium iodide (KI) (2% concentration) washbottles linked in series to break down any O_3 and a sodium thiosulfate ($Na_2S_2O_3$) washbottle also connected in series to trap any entrained I_2. The gas-phase O_3 concentration was determined by passing the stream through the bubbler (7537 special, 500 mL with Teflon stopcock and Teflon plug having a medium-pore glass diffuser; ACE Glass, Vineland, NJ) containing 2% KI solution at a known flow rate for a specified duration of time. The bubbler solution was next acidified with concentrated sulfuric acid and then titrated with standard $Na_2S_2O_3$ solution using starch solution as indicator. The amount of I_2 liberated from the KI solution was a direct measure of O_3 in the gas phase (Trivedi, 1992).

Ozone solubility in FC phase was determined by first saturating the fluorocarbon with ozone in the same glass bubbler. The glass bubbler was equipped with a frit to disperse ozonated oxygen into the fluorocarbon and a liquid outlet equipped with a Teflon stopcock to withdraw a sample of ozonated fluorocarbon, while the major portion of the fluorocarbon remained within the bottle. The exiting gases from the bubbler were passed into a washbottle filled with a KI solution to decompose unabsorbed ozone. The stopcock of the bubbler was then opened and a known volume of ozone-saturated fluorocarbon was brought in contact with known volume of freshly prepared KI solution (about 2%). After

Table 1. Properties of FC Liquids Used*

FC	Mol. Wt.	Boiling Point °C	Vapor† Pres. (mm. Hg)	Density† g/cm³	Kinem. Vis.† cs	Surface† Tension dyne/cm	Solub. of Water† ppm (wt.)	Solub. of FC in Water ppm
FC-43	670	174	1.3	1.88	2.8	16	7	ins.
FC-77	415	97	42.0	1.78	0.8	15	13	ins.

Product Manual (1989).
†Measured at 25°C; ins. = insoluble.

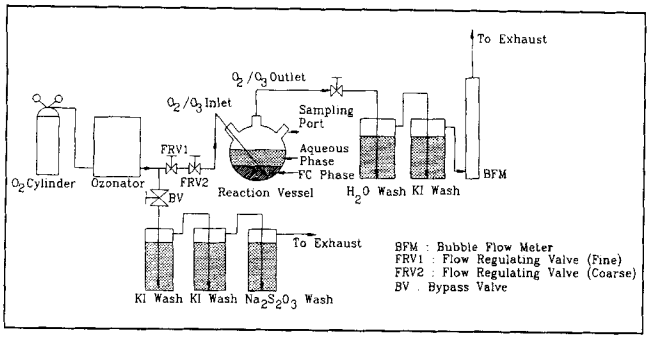

Figure 2. Experimental setup for determining ozonation degradation kinetics in the two-phase system operated under semibatch condition.

stirring the contents for about 15 min, a volume of 25 mL of the solution was acidified using a few drops of concentrated H_2SO_4 and the liberated iodine was titrated against standardized $Na_2S_2O_3$. The same amount (25 mL) of fresh KI solution was also titrated with $Na_2S_2O_3$ solution (after being acidified with H_2SO_4) to determine the blank concentration. The amount of I_2 liberated was a direct measure of O_3 present in the fluorocarbon sampled (Trivedi, 1992).

Degradation kinetics of pollutants in the two-phase system

The degradation kinetics of pollutants in the two-phase system was studied in two ways, by a semibatch method for toluene, TCE, and nitrobenzene, and by a batch method for phenol, acrylonitrile, and nitrobenzene. The *semibatch scheme* (Figure 2) involved a 100-mL glass vessel (ACE Glass, Vineland, NJ) having three ports capable of accepting 24 $40 glass fittings. Two ports were fitted with tube adapters (ACE Glass, Vineland, NJ); the third was covered with a rubber septum (Aldrich Chemical Co.). Chempruf Seamless TFE tubing (McMaster-Carr, New Brunswick, NJ) was used to complete the gas connections to and from the glass vessel. The gas inlet tube into the vessel was blocked and its sides were then pierced to achieve a better gas dispersion into the reaction medium. The gas leaving the vessel was passed through a wash bottle containing distilled water to pick up any organic compounds stripped from the reaction medium by the flowing gas and then through a washbottle containing KI to break down any unreacted ozone. Finally, at the outlet of the KI wash bottle, a bubble flowmeter was attached to monitor the gas-flow rate.

Known volumes of fluorocarbon and distilled water were taken in the reaction vessel and stirred, while ozonated oxygen was passed through them for half an hour. The stirring of the liquid mixture was stopped and the gas flow to the vessel was shut off while a known quantity of the pollutant was introduced into the reaction mixture. For compounds like TCE and toluene, a pure sample of the compound was injected into the FC phase, while an aqueous solution of nitrobenzene was pipetted into the vessel. After the pollutant was added, the two phases were kept well stirred and flow of ozonated oxygen through the reaction medium was resumed. The gas flow to the vessel and the stirring of the two phases were stopped while sampling the aqueous phase. In all experiments the washwater placed at the gas outlet from the reaction vessel did not show any trace of pollutants (Shanbhag, 1992).

When the setup was operated in the *batch mode*, a known volume of fluorocarbon was saturated with ozonated oxygen and an aqueous solution of the pollutant (acrylonitrile, phenol, and nitrobenzene) was then pipetted into the vessel. The gas inlet and exit valves to the vessel were shut off before pollutant was admitted to the vessel and the supply of ozonated oxygen to the vessel was not resumed after the addition of the pollutant as was done for the semibatch run. The sampling of the aqueous phase was identical to the method followed for the semibatch run. All studies were carried out at 25 ± 1°C.

Fabrication of membrane reactors

Geometrical characteristics of membrane reactors are presented in Table 2. Hydrophobic microporous polypropylene hollow fibers (Celgard X-10) were used to fabricate reactors 1 and 4. Reactors 2 and 3 were obtained from Hoechst Celanese (Liquid-Cel, Charlotte, NC). For reactor 5, microporous Teflon tubules (Impra, Tempe, AZ) were used as one set of tubules and the other set consisted of nonporous silicone capillaries (Dow Corning, Midland, MI). Fabrication procedure for all reactors was similar. Fabrication involved preparation of the fiber bundle, putting them in a shell and finally potting the ends with a resin mixture to form a tube sheet (Majumdar et al., 1988). For reactors 1, 4 and 5, two

Table 2. Geometrical Characteristics of Different Membrane Reactors

Reactor No.	Active Length cm	First Fiber Set Total No.	First Fiber Set ID/OD μm	Second Fiber Set Total No.	Second Fiber Set ID/OD μm	Void Space %	Surface Area/ Vol. cm^{-1}	Eff. Thickness* δ_m, μm
1†	43.2	300‡	100/150	300‡	100/150	63.7	48.4	123.2
2§	25.4	350‡	240/300	350‡	240/300	69.0	20.6	1,537
3§	25.4	350‡	240/300	350‡	240/300	69.0	20.6	320
4†	25.4	720‡	100/150	720‡	100/150	84.0	21.2	1,143
5†	20.8	48‖	304.8/635	6#	990/2,280	68.7	5.1	—

*Obtained from CO_2 permeation studies through water in such a module, (Majumdar et al., 1989). Actual FC-phase thickness will incorporate porosity and tortuosity of the fiber walls.
†Module fabricated.
‡Celgard X-10 hollow fiber; fiber bubble point pressure 1,034 kPa, mean pore size 0.03 μm.
§Modules obtained from Hoechst-Celanese.
‖Nonporous silicone capillaries.
#Microporous Teflon tubules.

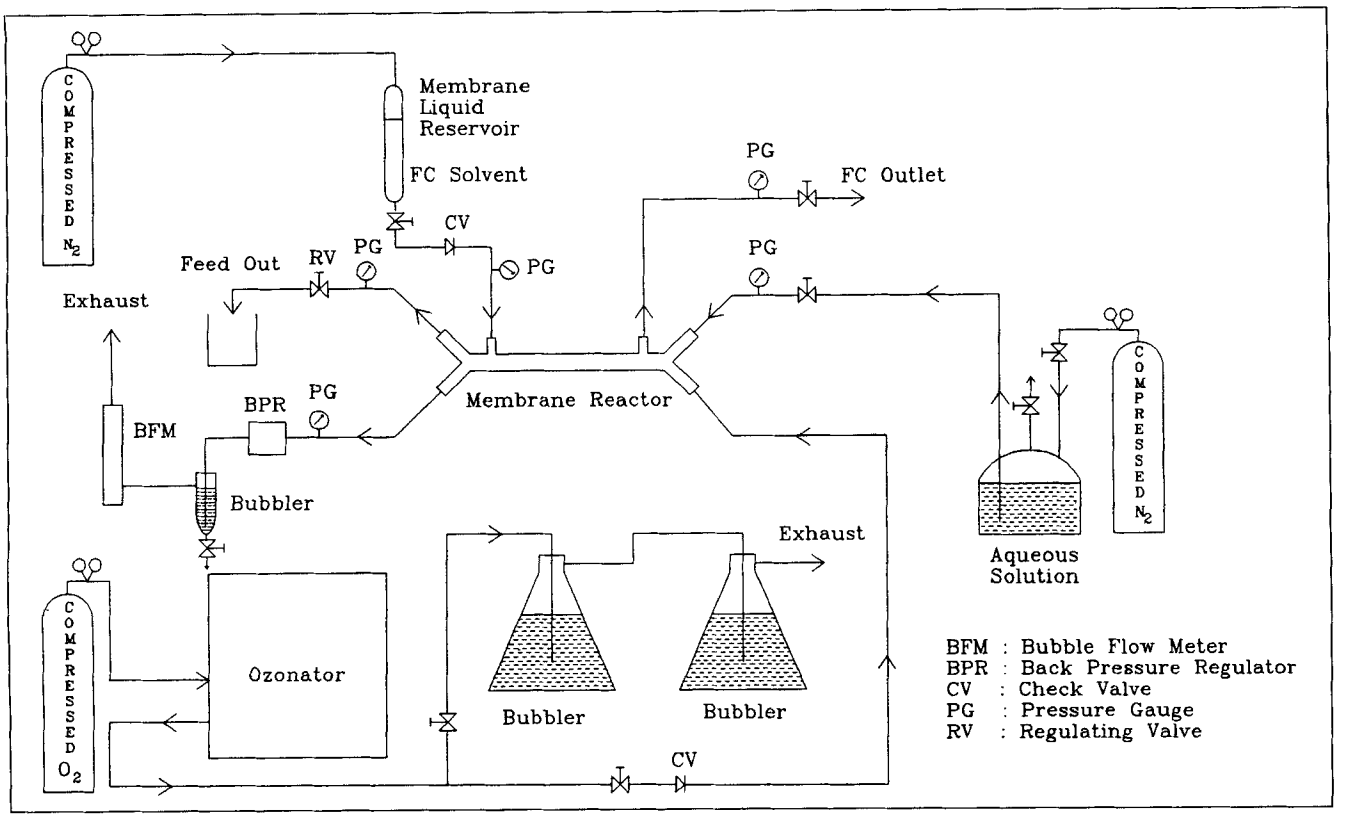

Figure 3. Experimental setup for ozonation in membrane reactor.

sets of hollow fibers (Teflon tubules and silicone capillaries for reactor 5) were placed in a transparent FEP shell (0.61 cm ID, 1.03 cm OD; Cole Parmer, Chicago) with polypropylene Y-fittings at the two ends. The fibers were potted using epoxies at the end of the Y-fittings. Armstrong epoxies (Beacon Chemical Co., Mt. Vernon, NY) C4-D was used for the internal tube sheet and A2-A for external hardening. The reactors (reactors 1 to 4) were characterized for effective fiber-to-fiber distance between two sets of fibers by gas permeation studies (Majumdar et al., 1989).

Degradation of pollutants in the membrane reactor

Ozonation of selected pollutants was carried out in a setup shown in Figure 3. The setup had three major sections all connected to the membrane reactor: an ozonator to supply ozone, a FC-liquid reservoir for the reaction medium, and an aqueous waste stream reservoir. As the ozonator output gas-flow rate is very high, the ozone-containing stream from the ozonator was split into two. One stream was bypassed through two bottles of KI wash and a bottle of thiosulfate wash to remove any O_3 before exhausting the gas to the hood. The other stream was passed through one set of fibers. Gas-side flow rate and pressure were controlled by a regulating (needle) valve placed at the exit end. The gas-side pressure was maintained at 115 kPa (2 psig). The spent gas stream was passed through a KI wash and then through a bubble flowmeter and finally to the exhaust hood. The synthetic aqueous waste stream was passed at a controlled rate and pressure through the other fiber set. The aqueous side pressure was maintained close to 115 kPa (2 psig). The FC liquid was admitted into the void space in the shell and maintained at atmospheric pressure. For reactor 5, the aqueous phase containing pollutant was allowed to flow through the bore of the Teflon tubules and the gas phase containing ozone was passed through the silicone capillaries. Since the silicone capillaries are nonporous, gas-side pressure could be raised, but was limited by the operating pressure of the ozone generator. The gas-side pressure was maintained at 115 kPa (2 psig). The exiting aqueous phase pollutant concentration was measured by the HPLC at suitable time intervals. Experiments were carried out at 25 ± 1°C.

A Model for Batch and Semibatch Ozonation Kinetics in a Two-phase System

Ozonation of a pollutant in a two-phase batch system is shown in Figure 4. The reaction between the pollutant (A) and ozone (B) can occur in the aqueous phase (Eq. 2) as well as in the organic phase (Eq. 3):

$$a'A(W) + b'B(W) \rightarrow \text{products } (W) \qquad (2)$$

$$aA(F) + bB(F) \rightarrow \text{products } (F). \qquad (3)$$

Here a and b are the stoichiometric coefficients for organic phase oxidation; a' and b' are the corresponding values for aqueous phase oxidation. Three basic assumptions have been made in deriving the kinetic model: (a) each phase is well mixed; (b) both phases are always at distribution equilibrium for any species; and (c) the removal of the pollutant by strip-

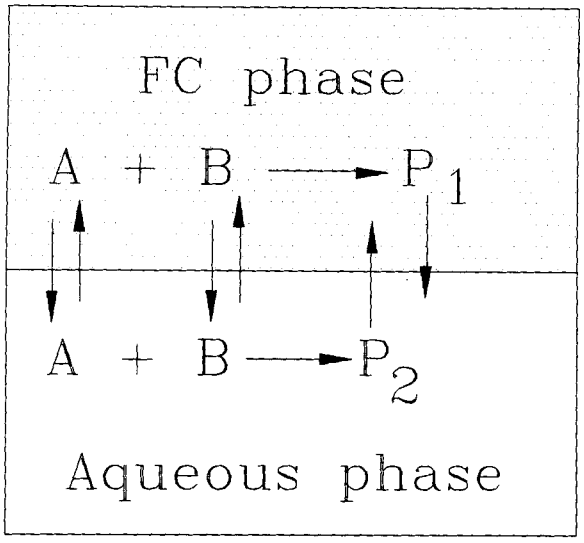

Figure 4. Batch reaction mechanism.

ping and vaporization is negligible. Assuming second-order kinetics, an overall material balance for the disappearance of A may be written as

$$-V^F\frac{dC_A^F}{dt}-V^W\frac{dC_A^W}{dt}=k_2^F C_A^F C_B^F V^F+k_2^W C_A^W C_B^W V^W \quad (4)$$

At $t=0$, $C_A^W=C_{A0}^W=C_{A0}^F/m_A$; $m_A=C_A^F/C_A^W$ at any time t (5)

At $t=0$, $C_B^W=C_{B0}^W=C_{B0}^F/m_B$; $m_B=C_B^F/C_B^W$ at any time t. (6)

Therefore Eq. 4 can be rewritten as

$$(m_AV^F+V^W)\left(-\frac{dC_A^W}{dt}\right)=(k_2^F m_A m_B V^F+k_2^W V^W)C_A^W C_B^W. \quad (7)$$

Further assuming the same stoichiometry in both phases, an overall material balance can be written as follows

$$V^F(C_{A0}^F-C_A^F)+V^W(C_{A0}^W-C_A^W)=\frac{a}{b}[V^F(C_{B0}^F-C_B^F)+V^W(C_{B0}^W-C_B^W)]. \quad (8)$$

One can express C_B^W from Eq. 8 as

$$C_B^W=C_{B0}^W-\frac{b}{a}\frac{(m_AV^F+V^W)}{(m_BV^F+V^W)}(C_{A0}^W-C_A^W) \quad (9)$$

where C_{B0}^W is the initial saturation concentration of ozone in the aqueous phase in equilibrium with the saturation concentration of ozone in the FC phase, C_{B0}^F.

Define a second-order rate constant k_2^{eff} such that

$$(k_2^F m_A m_B V^F+k_2^W V^W)=k_2^{\text{eff}}(m_A m_B V^F+V^W). \quad (10)$$

Combining Eqs. 7, 9 and 10, a pollutant material balance can be obtained as

$$-\frac{dC_A^W}{dt}=k_2^{\text{eff}}\frac{(m_Am_BV^F+V^W)}{(m_AV^F+V^W)}C_A^W \times\left(C_{B0}^W-\frac{b}{a}\frac{(m_AV^F+V^W)}{(m_BV^F+V^W)}(C_{A0}^W-C_A^W)\right). \quad (11)$$

Grouping terms together and integrating between appropriate limits yield

$$-\int_{C_{A0}^W}^{C_A^W}\frac{dC_A^W}{C_A^W(M_1+N_1C_A^W)}=\int_0^t\frac{k_2^{\text{eff}}dt}{R_1} \quad (12)$$

where

$$M_1=C_{B0}^W-\frac{b}{a}\frac{(m_AV^F+V^W)}{(m_BV^F+V^W)}C_{A0}^W \quad (13)$$

$$N_1=\frac{b}{a}\frac{(m_AV^F+V^W)}{(m_BV^F+V^W)} \quad (14)$$

$$R_1=\frac{m_AV^F+V^W}{(m_Am_BV^F+V^W)}. \quad (15)$$

This yields the analytical solution

$$-\frac{1}{M_1}\ln\left(\frac{C_A^W}{M_1+N_1C_A^W}\right)\Bigg|_{C_{A0}^W}^{C_A^W}=\frac{k_2^{\text{eff}}t}{R_1}\Bigg|_0^t. \quad (16)$$

This is a general rate expression for the degradation of a pollutant in a two-phase system. The pollutant concentration in the aqueous phase thus depends among others on the volumes of the solvent and the aqueous phase, the pollutant partition coefficient, and the stoichiometric ratio of the two reactants. Extricating information about k_2^{eff} and b/a would require curve-fitting this equation to experimental information of C_A^W vs. t. These values of b/a and k_2^{eff} may be quite different from those for aqueous phase ozonation since the exact reaction pathways in the FC phase and the degradation kinetics in this biphasic system are not known.

A simplification can be made if it is assumed that the rate of destruction of the pollutant in the organic phase dominates the overall reaction kinetics. Then the second term on the righthand side of Eq. 4 can be neglected. Moreover, since the concentration of ozone in the aqueous phase is very low, the extent of the oxidative degradation in the aqueous phase would be much smaller than that in the organic phase. We can express C_B^F now as

$$C_B^F=C_{B0}^F-\frac{b}{a}(C_{A0}^F-C_A^F) \quad (17)$$

where C_{A0}^F is the pollutant concentration in the FC-phase in equilibrium with the aqueous phase at the start of the experiment (this is obtained from mass balance and an estimate of the partition coefficient known *a priori*). This yields the analytical solution

$$-\frac{1}{M_2}\ln\left(\frac{C_A^W}{M_2+N_2C_A^W}\right)\Bigg|_{C_{A0}^W}^{C_A^W}=\frac{k_2^F t}{R_2}\Bigg|_0^t \tag{18}$$

where

$$M_2=C_{B0}^F-m_A\frac{b}{a}C_{A0}^W \tag{19}$$

$$N_2=m_A\frac{b}{a} \tag{20}$$

$$R_2=\frac{m_AV^F+V^W}{m_AV^F}. \tag{21}$$

A further simplification may be made if O_3 concentration in the FC phase is in large excess compared to that of the pollutant; a modification of Eq. 4 can be used where the product of k_2^F and C_B^F gives a pseudo-first-order rate constant k_1^F. Assuming that all of the reaction occurs in the FC phase, the material balance is modified as

$$-V^F\frac{dC_A^F}{dt}-V^W\frac{dC_A^W}{dt}=k_1^FC_A^FV^F. \tag{22}$$

Rewrite this equation as

$$-\frac{dC_A^W}{dt}=\frac{k_1^Fm_AV^FC_A^W}{(m_AV^F+V^W)}. \tag{23}$$

Integration leads to

$$\ln\frac{C_A^W}{C_{Ao}^W}=-\left(\frac{k_1^Fm_AV^F}{m_AV^F+V^W}\right)t. \tag{24}$$

This relation [similar to the pseudo-first-order analysis by Stich and Bhattacharyya (1987)] can be used to determine the pseudo-first-order reaction rate constant for an individual pollutant using m_A and the volumes of the solvent and water.

A Kinetic Model for the Membrane Reactor

The general phenomena at any axial location of the membrane reactor are shown in Figure 5. Here aqueous phase containing a pollutant flows through the lumen of one set of fibers and ozonated oxygen flows through the other set of fibers. Stagnant fluorocarbon phase acts as an inert reaction medium in between the two phases. Ozone from the gas-phase partitions into the FC phase at the gas–FC interface for microporous membranes (Figure 1a). Pollutant from the aqueous phase will diffuse through the aqueous boundary layer, partition into the FC phase in the fiber pores, and then finally diffuse through the bulk of the FC phase while reacting with O_3. Concentration profiles of ozone and pollutant at any axial location will be influenced by the distribution coefficient, diffusivity, and the reaction rate constant.

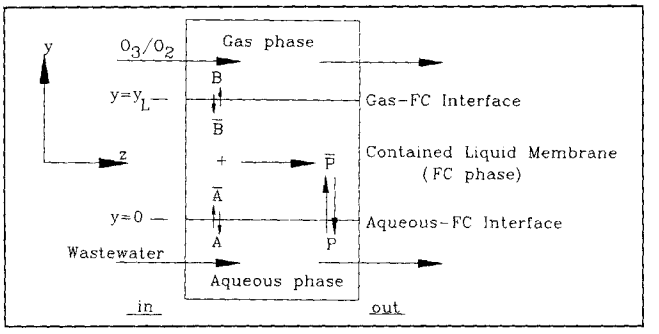

Figure 5. Reaction mechanism in the membrane reactor.

The assumptions used to develop a kinetic model for this reactor are:

(1) Axial diffusion in the stationary liquid FC film is neglected.

(2) A constant effective FC-phase thickness y_L is assumed throughout the length of the reactor as well as at all radial locations in the reactor.

(3) Reaction occurs only in the FC phase.

(4) The rate of stripping of pollutants into the gas phase is negligible.

The governing diffusion-reaction equations at any axial location in the FC phase for the pollutant (A) and ozone (B) are

$$\bar{D}_A\frac{d^2\bar{C}_A}{dy^2}=k_2^F\bar{C}_A\bar{C}_B \tag{25}$$

$$\bar{D}_B\frac{d^2\bar{C}_B}{dy^2}=\left(\frac{b}{a}\right)k_2^F\bar{C}_A\bar{C}_B \tag{26}$$

Boundary Conditions:

$$\text{at } y=0 \quad \bar{C}_A=\bar{C}_{Ai}; \qquad \frac{d\bar{C}_B}{dy}=0 \tag{27}$$

$$\text{at } y=y_L \quad \frac{d\bar{C}_A}{dy}=0; \qquad \bar{C}_B=\bar{C}_{Bi}. \tag{28}$$

This is a boundary value problem and no analytical solution is available.

For pollutants having a low to moderate m_A, assume O_3 concentration to be uniform and in large excess compared to that of the pollutant. Then Eq. 25 is simplified to

$$\bar{D}_A\frac{d^2\bar{C}_A}{dy^2}=k_1^F\bar{C}_A \tag{29}$$

where the pseudo-first-order rate constant k_1^F is given by the product of k_2^F and $\bar{C}_B$.

Integration (Froment and Bischoff, 1979) leads to

$$\bar{C}_A = A_1 \text{Cosh}\left(\gamma \frac{y}{y_L}\right) + A_2 \text{Sinh}\left(\gamma \frac{y}{y_L}\right) \tag{30}$$

$$\text{where } \gamma = \text{Hatta Number} = \frac{\sqrt{k_1^f \bar{D}_A}}{\bar{k}}. \tag{31}$$

Here y_L is defined via

$$\frac{1}{\bar{k}} = \frac{y_L}{\bar{D}_A} = \frac{d_i}{d_{lm}} \frac{\tau(d_o - d_i)}{\bar{D}_A \epsilon} + \frac{d_i}{d_o} \frac{1}{\frac{\bar{D}_A}{\delta_m}}, \tag{32}$$

which takes into account the diffusion in the pores in the hollow fiber wall along with that in the stagnant FC liquid of thickness δ_m in the shell side.

Boundary conditions for Eq. 30 are

$$\text{at } y = 0 \quad \bar{C}_A = \bar{C}_{Ai}; \qquad \text{at } y = y_L \quad \bar{C}_A = 0. \tag{33}$$

Using the conditions in Eq. 33, constants A_1 and A_2 of Eq. 30 are evaluated. The final concentration profile $\bar{C}_A$ and the radial flux of A are, respectively,

$$\bar{C}_A = \bar{C}_{Ai} \frac{\text{Sinh}\,\gamma\left(1 - \frac{y}{y_L}\right)}{\text{Sinh}\,\gamma} \tag{34}$$

$$N_{Ay} = -\bar{D}_A \left[\frac{d\bar{C}_A}{dy}\right]_{y=0} = \frac{\gamma \bar{D}_A \bar{C}_{Ai}}{y_L \tanh\gamma}. \tag{35}$$

Radial pollutant flux across the aqueous boundary layer can also be written in terms of a concentration difference as

$$N_{Ay} = k_w(C_{Ab}^W - C_{Ai}^W) = k_w\left(C_{Ab}^W - \frac{\bar{C}_{Ai}}{m_A}\right). \tag{36}$$

The aqueous-side mass-transfer coefficient k_w is obtained from the Graetz solution (Skelland, 1974; Prasad and Sirkar, 1988). Equations 35 and 36 provide the pollutant flux expression

$$N_{Ay} = \left(\frac{\gamma \bar{D}_A m_A C_{Ab}^W}{y_L \tanh\gamma}\right) \Bigg/ \left(1 + \frac{\gamma \bar{D}_A m_A}{y_L k_w \tanh\gamma}\right). \tag{37}$$

For the pollutant concentration change along module length, one can write

$$-\left(\frac{Q_w}{\pi d_i N_{FT}}\right) \frac{dC_{Ab}^W}{dz} = \left(\frac{\gamma \bar{D}_A m_A C_{Ab}^W}{y_L \tanh\gamma}\right) \Bigg/ \left(1 + \frac{\gamma \bar{D}_A m_A}{y_L k_w \tanh\gamma}\right). \tag{38}$$

If k_w does not vary with the reactor length, a simplified result is obtained by integrating Eq. 38 using boundary conditions at $z = 0$, $C_{Ab}^W = C_{Ab}^W|_{\text{in}}$ and at $z = L$, $C_{Ab}^W = C_{Ab}^W|_{\text{out}}$

$$C_{Ab}^W|_{\text{out}} = C_{Ab}^W|_{\text{in}} \exp\left(-\frac{\frac{\gamma \bar{D}_A m_A}{y_L \tanh\gamma}}{1 + \frac{\gamma \bar{D}_A m_A}{y_L k_w \tanh\gamma}} \left(\frac{\pi d_i N_{FT} L}{Q_w}\right)\right). \tag{39}$$

Conversion in such a reactor is defined as

$$X_A = \frac{C_{Ab}^W|_{\text{in}} - C_{Ab}^W|_{\text{out}}}{C_{AB}^W|_{\text{in}}}. \tag{40}$$

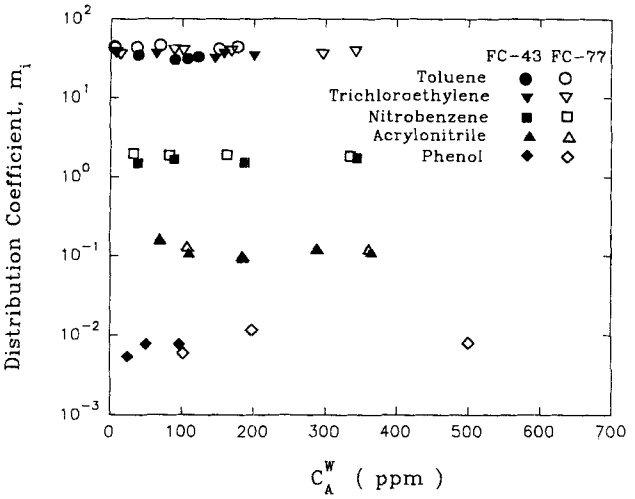

Figure 6. Distribution coefficient of pollutants between FC and aqueous phases.

Results and Discussion

The results are presented and discussed in the following order: pollutant distribution coefficient studies, batch and semibatch ozonation kinetic studies, and membrane reactor studies. Results of model simulations are also provided for batch kinetic studies and the membrane reactor degradation of pollutants.

Distribution coefficients/solubilities

Experimental values of distribution coefficients of different pollutants between aqueous and different FC phases are shown in Figure 6 as a function of the aqueous phase pollutant concentration. The m_A values appear to be essentially independent of the solute concentration in this low range thus satisfying Nernst distribution law. It is also evident that hydrophobic compounds like toluene, TCE have much higher distribution coefficients compared to those for phenol and acrylonitrile, while m_A for nitrobenzene falls in between this range of values. Solubilities of ozone in FC-43 and FC-77 were found to be 78 mg/L and 125 mg/L, respectively. These

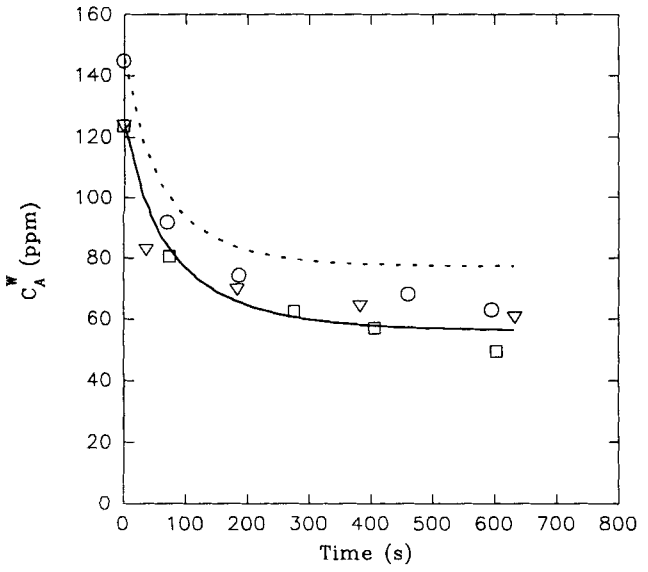

Figure 7a. Concentration vs. time for degradation of phenol in batch mode: experimental data and simulation results based on second-order reaction rate model.

FC77: Water = 30 mL: 50 mL; $k_2^{eff} = 40\ M^{-1}s^{-1}$, $b/a = 2$; ▽ □ $C_{AO}^W = 124$ ppm; —— simulation; ○ $C_{AO}^W = 146$ ppm; ----- simulation.

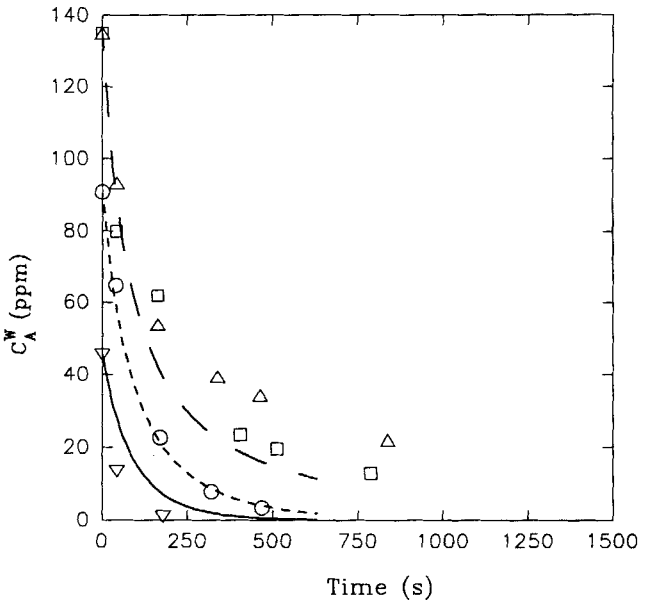

Figure 8a. Concentration vs. time plot for degradation of acrylonitrile in batch mode: experimental data and simulation results based on second-order reaction rate model.

FC77: Water = 30 mL: 50 mL; $k_2^{eff} = 40\ M^{-1}\ s^{-1}$; $b/a = 0.5$; ▽ $C_{AO}^W = 45$ ppm; —— simulation; ○ $C_{AO}^W = 91$ ppm; ------ simulation; □ △ $C_{AO}^W = 135$ ppm; ---- simulation.

values are much higher compared to the solubility of ozone in water, which was reported to be 11.8 ppm (Langlais et al., 1991) at 25°C.

Batch/semibatch two-phase ozonation kinetics

Results of *batch* kinetics experiments for pollutants phenol, acrylonitrile, and nitrobenzene having low to moderate partition coefficients into the FC phase are presented in Figures 7 to 9 respectively. The FC-77:water ratio used in all cases was 30:50. Using Eq. 16 for each compound, the experimental values of C_A^W as a function of time have been curve fitted to yield the best estimates of k_2^{eff} that describe the data for different $C_{AO}^W s$ for an assumed value of (b/a). The values of k_2^{eff} and (b/a) are indicated in each of Figures 7a, 8a and

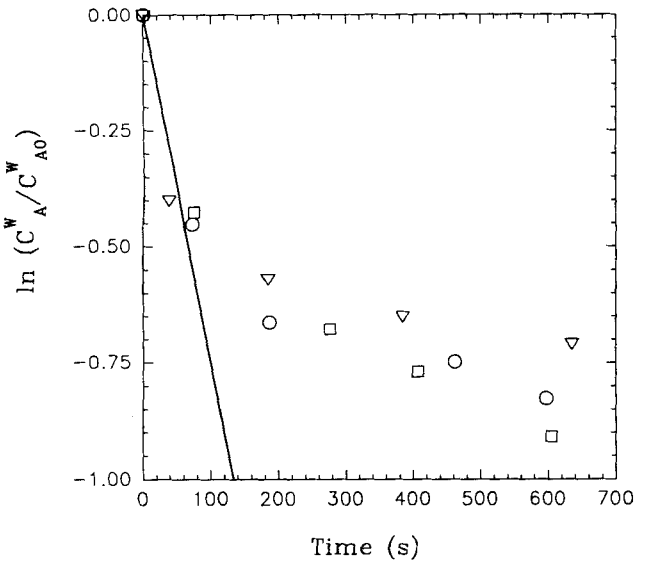

Figure 7b. Degradation of phenol in batch mode: experimental data and simulation results based on pseudo-first-order reaction kinetics.

FC77: Water = 30 mL: 50 mL; $k_1^F = 1.0\ s^{-1}$, ▽ □ $C_{AO}^W = 124$ ppm; ○ $C_{AO}^W = 146$ ppm.

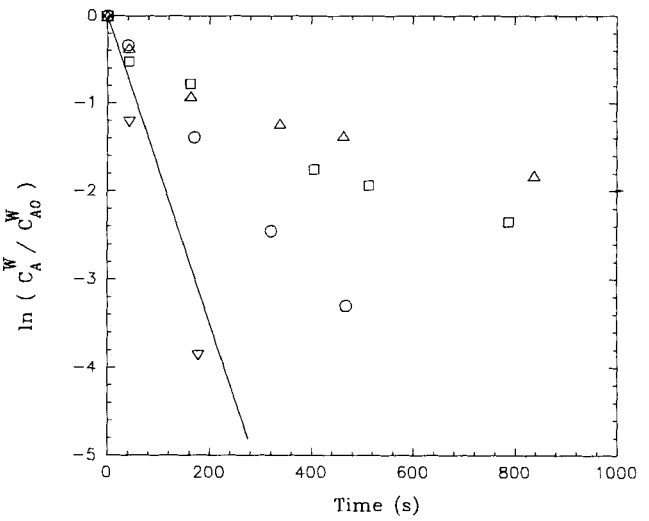

Figure 8b. Degradation of acrylonitrile in batch mode: experimental data and simulation results based on pseudo-first-order reaction kinetics.

FC77: Water = 30 mL: 50 mL; $k_1^F = 0.26\ s^{-1}$; ▽ $C_{AO}^W = 45$ ppm; ○ $C_{AO}^W = 91$ ppm; □ △ $C_{AO}^W = 135$ ppm.

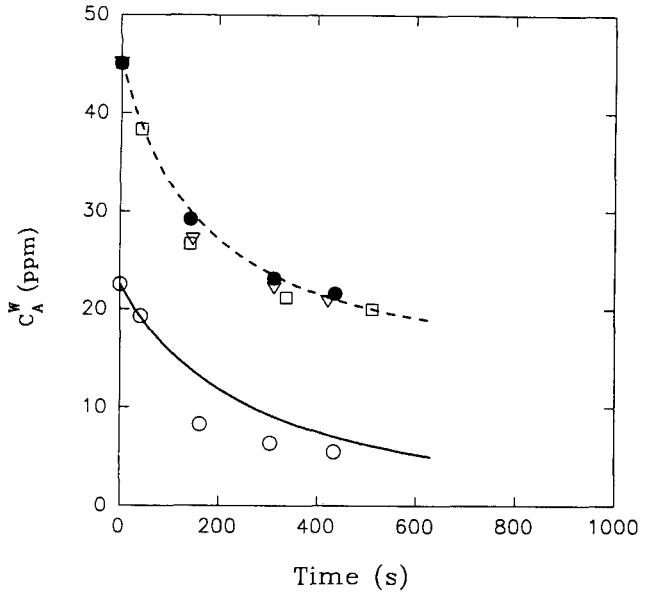

Figure 9a. Concentration vs. time plot for degradation of nitrobenzene in batch mode: experimental data and simulation results based on second-order reaction rate model.

FC77: Water = 30 mL: 50 mL; $k_2^{eff} = 3.5\ M^{-1}s^{-1}$; $b/a = 3.0$; ○ $C_{AO}^W = 23$ ppm; —— simulation; ▽ □ ● $C_{AO}^W = 45$ ppm; ------ simulation.

9a. It appears that the second-order model is quite effective in describing the observed behavior. The value of (b/a) should depend upon the type of pollutant and the reaction environment. In aqueous phase ozonation, the value of the stoichiometric ratio lies between 1 and 5 (Hoigné and Bader, 1983).

The relevance of the pseudo-first-order rate model in *batch* ozonation kinetics has been explored for the same pollutants

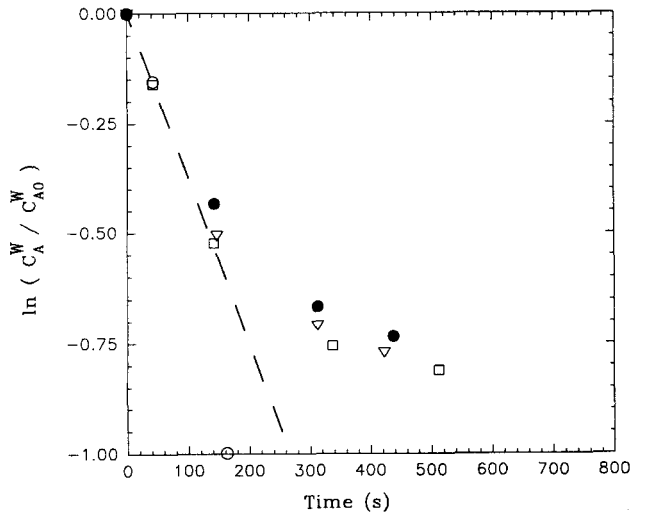

Figure 9b. Degradation of nitrobenzene in batch mode: experimental data and simulation results based on pseudo-first-order reaction kinetics.

FC77: Water = 30 mL: 50 mL; $k_1^F = 7.0 \times 10^{-3}\ s^{-1}$; ○ $C_{AO}^W = 23$ ppm; ▽ □ ● $C_{AO}^W = 45$ ppm.

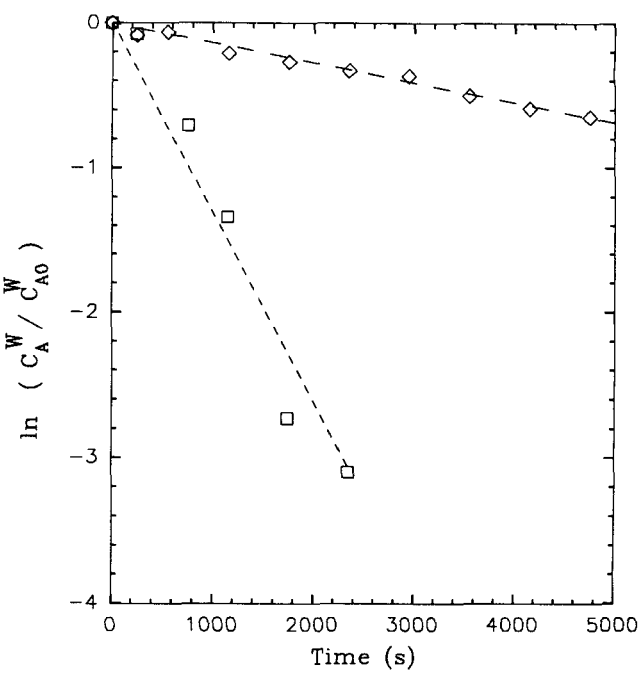

Figure 10. Degradation of organic compounds in semibatch mode: experimental data and simulation results based on pseudo-first-order reaction kinetics.

---, ◇ Toluene; $C_{AO}^W = 57$ ppm; $k_1^F = 1.39 \times 10^{-4} s^{-1}$; FC77: Water = 50 mL: 30 mL; ozone dosage rate = 1.1 mg/min; total amount of toluene = 0.13 gm; ----, □ TCE; $C_{AO}^W = 36$ ppm; $k_1^F = 1.32 \times 10^{-3} s^{-1}$; FC77: Water = 50 mL: 30 mL; ozone dosage rate = 0.96 mg/min; total amount of TCE = 0.073 gm.

by plotting ln (C_A^W/C_{A0}^W) vs. time for each pollutant in Figures 7b, 8b, and 9b. A line was drawn through the initial set of data points and the origin; the slope of this line was used to calculate the first-order reaction rate constant k_1^F from Eq. 24. For pollutants having a low distribution coefficient up to around 1, at the beginning there would be excess ozone in the FC phase, and the pollutant degradation rate exhibited pseudo-first-order kinetics. However, this trend will be strictly dictated by the initial equilibrium aqueous phase concentration. This is evinced in Figures 7b to 9b, where the initial change in aqueous phase pollutant concentration showed a linear profile and the profile veers away from pseudo-first-order behavior to a higher order reaction regime, more rapidly, as the initial equilibrium aqueous phase concentration of a pollutant is increased.

The depletion of ozone by reaction in a *batch* system may be avoided by the *semibatch* ozonation technique with a constant supply of ozonated air especially for pollutants having a high m_A. Results of semibatch ozonation for pollutants like TCE and toluene having high partition coefficients into the FC-phase are shown in Figure 10 in the form of ln (C_A^W/C_{A0}^W) vs. time. Linear plot of ln (C_A^W/C_{A0}^W) vs. time suggest that pseudo-first-order kinetics describe the data well for each pollutant. The pseudo-first-order reaction rate constants obtained for each of these compounds were found to be a few times higher than those obtained for simple aqueous ozonation (such as for TCE, Table 4, Glaze and Kang (1988), obtained $4.1 \times 10^{-4}\ s^{-1}$ as the pseudo-first-order degradation

coefficient in the absence of any alkalinity and H_2O_2; the first-order degradation coefficient was found here in the absence of any alkalinity to be 1.33×10^{-3} s^{-1}). At the end of the experiment for the semibatch degradation of TCE, the Cl^- ion concentration observed in the aqueous phase was 1,121 ppm, indicating that more than half of the TCE present had been mineralized to HCl.

Figure 10 also illustrates the relative ease with which compounds such as TCE and toluene can be degraded. TCE, an unsaturated compound, is easier to degrade than toluene. The presence of the aqueous phase in intimate contact with the organic phase allows the possibility of another reactant to enhance the degradation, for example, to enhance the mineralization of TCE, the presence of an alkali in the aqueous phase may aid the process by scavenging the H^+ ions released by the reaction.

The ratio of FC:water in these experiments was chosen such that there was an adequate amount of ozone within the liquid medium to degrade the pollutant (especially for pollutants having a high m_A), and to ensure that not all the pollutant disappeared just by simple extraction into the fluorocarbon phase. For pollutants having a high m_A into the FC phase, the FC has another attractive characteristic, that is, it acts as an extracting solvent, especially in the case of pollutants like TCE and toluene. If one were to consider the semibatch data for, say, toluene, the equilibrium aqueous phase concentration of toluene at the start of the reaction was reported to be 57 ppm; the equilibrium concentration of toluene in the FC phase would then be in the range of 2,200 mg/L. Therefore if FC were brought into contact with industrial wastewater containing toluene at concentration levels of 100 to 150 ppm, the high partition coefficient of toluene into the FC phase would result in an immediate reduction of the aqueous-phase toluene concentration. Toluene would then be essentially subject to degradation by ozone with the FC phase. A similar situation would cause the enhanced degradation of TCE by ozone in the presence of the FC phase. The values of pseudo-first-order rate constant obtained from batch and semibatch studies are summarized in Table 3.

A comparison of the pseudo-first-order degradation constants between those obtained experimentally and those found in the literature are also shown in Table 3. The pseudo-first-order degradation constants obtained from the literature were those where ozonated oxygen was used in direct contact with wastewater in the absence of any reaction catalyzing agents. From Table 3 it is clear that for the degradation of phenol and TCE, the proposed two-phase ozonation does offer considerably higher reaction rate constants as opposed to direct ozonation (Joshi and Shambaugh, 1982; Glaze and Kang, 1988). In the case of toluene where H_2O_2 and UV were used, the degradation constant obtained experimentally was less than that obtained from the literature, although the total amount of pollutant that was degraded in the two-phase system was higher (the total amount would be the amount present in the aqueous phase and that present in the FC phase).

Table 3. Comparison of Experimental k_1^F with k_1^W from the Literature

Pollutant	m_A	C_{A0}^W ppm	k_1^F, s^{-1} Present Study	k_1^W, s^{-1} Literature
Phenol	0.01	124–146	$1.26^{\dagger}$	$9.6\times10^{-2**}$
Acrylonitrile	0.12	45–135*	$0.26^{\ddagger}$	—
Nitrobenzene	1.9	23–45*	$7.0\times10^{-3\S}$	—
TCE	40	36*	$1.33\times10^{-3\|\|}$	$4.1\times10^{-4\dagger\dagger}$
Toluene	45	57*	$1.39\times10^{-4\#}$	$1.57\times10^{-3\ddagger\ddagger}$

*Equilibrium aqueous phase concentration calculated from distribution coefficient values (m_i).
$^{\dagger}k_1^F$ from Figure 7b.
$^{\ddagger}k_1^F$ from Figure 8b.
$^{\S}k_1^F$ from Figure 9b.
$^{\|}k_1^F$ from Figure 10, Ozone dosage rate = 0.96 mg/min.
$^{\#}k_1^F$ from Figure 10, Ozone dosage rate = 1.1 mg/min.
**Joshi and Shambaugh (1982).
††Table 4, Glaze and Kang (1988), (Ozone dosage rate = 4.6 mg/min).
‡‡Sundstrom et al. (1989), (UV and H_2O_2).
m_A = defined by Eq. 1.

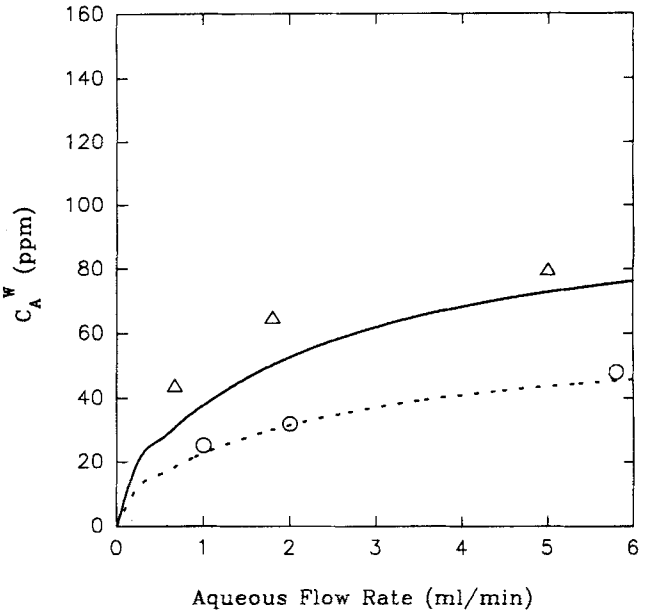

Figure 11. Degradation of phenol in membrane reactor 3 for different aqueous phase flow rates: experimental data and simulation results based on pseudo-first-order reaction kinetics in the membrane phase.

Gas flow rate 100 mL/min., Data: ○ 60 ppm feed; △ 100 ppm feed; —— simulation, 60 ppm; $k_1^F = 1\ s^{-1}$; $y_L = 1{,}193$ μm; – – simulation, 100 ppm; $k_1^F = 1\ s^{-1}$; $y_L = 1{,}193$ μm.

Performances of membrane reactors

The results of degradation of different pollutants in different membrane reactors are presented next. Figure 11 shows the steady-state degradation of phenol in reactor 3 for 60 ppm and 100 ppm feed aqueous phase concentrations for different aqueous phase flow rates. Significant degradation was observed at low aqueous phase flow rates. The aqueous phase residence time in the reactor was around 5 min for the lowest feed flow rate. The system reached steady state within 10 to 30 min, depending on the aqueous phase flow rate. The simulation results were plotted based upon a pseudo-first-order reaction model for degradation of the pollutant in the FC phase. The parameters used for simulation are presented in Table 4 where y_L for each reactor was calculated from Eq. 32. The diffusivities of individual pollutants in aqueous and

Table 4. Parameters Used for Simulation of Pollutant Degradation in Membrane Reactor

Pollutant	m_A	k_1^F, s^{-1}	k_2^{eff}, $M^{-1} \cdot s^{-1}$	$(b/a)^*$	$D_A^{W\dagger} \times 10^5$, cm^2/s	$D_A^{F\dagger} \times 10^5$, cm^2/s	$y_L^{\ddagger}$, μm
Phenol	0.01	1.26	40.0	2.0	0.91	2.2	1,193[§]
Acrylonitrile	0.12	0.26	40.0	0.5	1.16	2.32	1,472[‖]
Nitrobenzene	1.9	0.007	3.5	3.0	0.84	1.62	1,472[‖]
TCE	40	—	—	—	0.98	2.05	—
Toluene	45	—	—	—	0.86	1.8	—

*Stoichiometric ratio (moles of ozone/mole of pollutant).
†Diffusivities of solutes in aqueous and FC phase calculated from the Wilke–Chang correlation (Perry and Green, 1984).
‡From Eq. 32.
§For Reactor 3.
‖For Reactor 4.

FC phases were calculated using the Wilke–Chang equation (Perry and Green, 1984). The pseudo-first-order-based simulation appears to predict the performance for phenol quite well. Note that the low distribution coefficient of phenol in the FC phase will create an excess ozone condition in that phase. Therefore flux at any local position of the reactor is controlled mostly by the boundary layer resistance of the aqueous phase. Since the Hatta number is greater than 3, the enhancement factor in the FC phase always approaches the maximum value of γ as tanh γ becomes unity. The k_1^F value used to simulate the degradation of phenol in the membrane reactor was 1.0 s^{-1}. The value of y_L used in the simulation was 1,193 μm. Simulations for acrylonitrile and nitrobenzene are not shown because the pseudo-first-order model could not predict the degradation of the pollutant in the reactor well.

The degradations of nitrobenzene, acrylonitrile, and toluene were studied in different membrane reactors, and the steady-state performances are shown in Figures 12 and 13. The systems reach steady state within 20 min. These demonstrate the ability of such a reactor configuration to treat wastewater containing these compounds. However, the fine fibers of polypropylene (providing such a huge surface area per unit volume) were degraded by the high O_3 concentration in the FC phase (relative to water). The variations of pertinent parameters like gas flow rate, liquid flow rate, and pollutant loading levels could not be studied in such a reactor.

The results of degradation studies using the much more rugged membrane reactor 5 for pollutants like phenol, acrylonitrile, nitrobenzene, trichloroethylene, and toluene are presented in Figures 14 and 15. Figure 14 shows the results of variation of the conversion of each of the five pollutants with the aqueous flow rate in the reactor, while Figure 15 illustrates the effect of variation of gas flow rate on the conversion in the reactor for pollutants, phenol, and toluene only. For the lowest aqueous flow rate, the residence time in the reactor was about 10 min.

For the degradation of phenol in the membrane reactor,

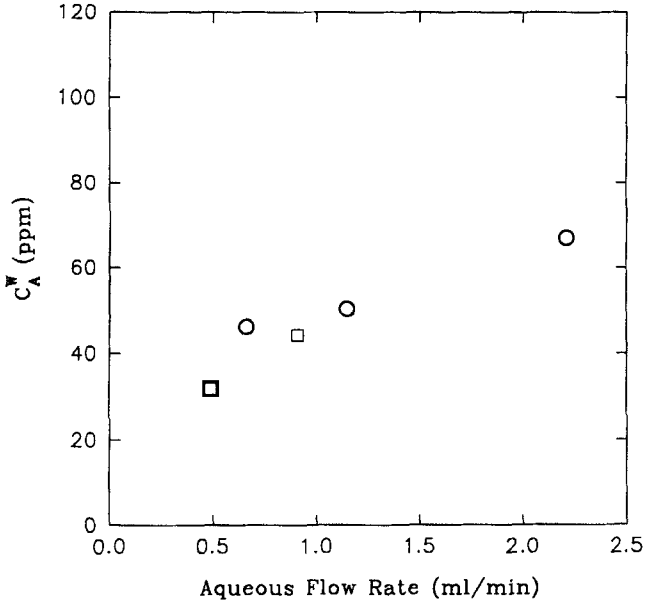

Figure 12. Degradation of pollutants in membrane reactor 4: effects of aqueous phase flow variations, FC used FC77.

○ Nitrobenzene; $C_{A0}^W = 100$ ppm; gas flow rate = 50 mL/min; □ Acrylonitrile; $C_{AO}^W = 96$ ppm; gas flow rate = 90 mL/min.

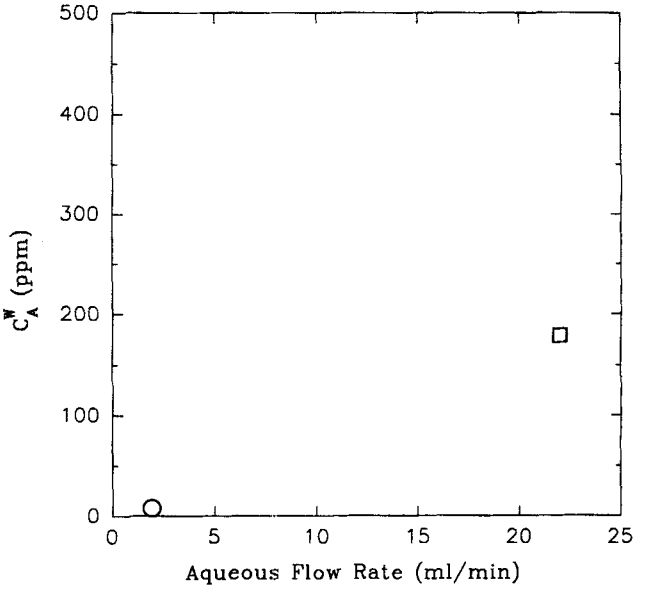

Figure 13. Degradation of toluene in membrane reactors 1 and 2 at different aqueous phase flow rates.

Gas flow rate = 50 mL/min. □ Reactor 2, FC43; C_{AO}^W = 391 ppm; ○ Reactor 1, FC77; $C_{AO}^W = 415$ ppm.

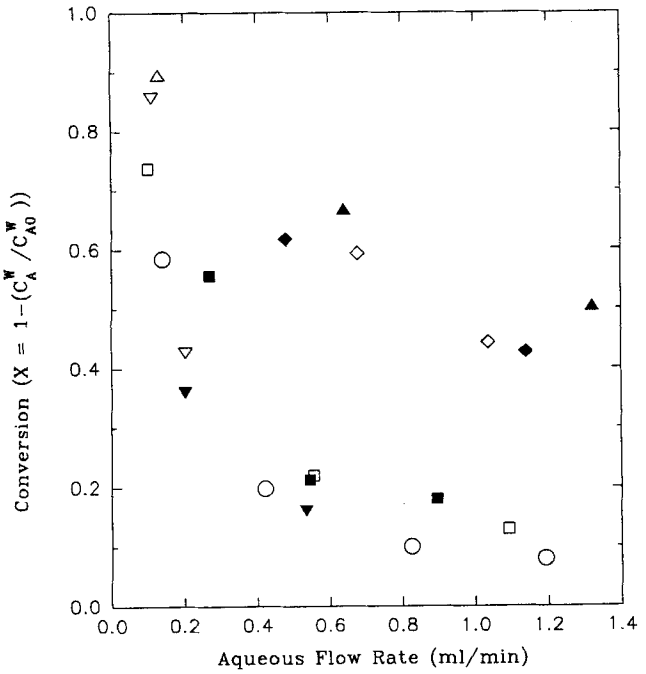

Figure 14. Degradation of various pollutants in membrane reactor 5: effects of aqueous phase flow variations on conversion, for FC43.

Phenol: ○ $C_{AO}^W = 152$ ppm; gas flow rate = 30 mL/min. **Acrylonitrile:** ▽ $C_{AO}^W = 160$ ppm; gas flow rate = 28 mL/min; ▼ $C_{AO}^W = 156$ ppm; gas flow rate = 27 mL/min. **Nitrobenzene:** □ $C_{AO}^W = 117$ ppm; gas flow rate = 33 mL/min; ■ $C_{AO}^W = 166$ ppm; gas flow rate = 31 mL/min. **Toluene:** △ $C_{AO}^W = 100$ ppm; gas flow rate = 28 mL/min; ▲ $C_{Ao}^W = 121$ ppm; gas flow rate = 28 mL/min. **TCE:** ◇ $C_{AO}^W = 83$ ppm; gas flow rate = 25 mL/min; ◆ $C_{AO}^W = 66$ ppm; gas flow rate = 22 mL/min.

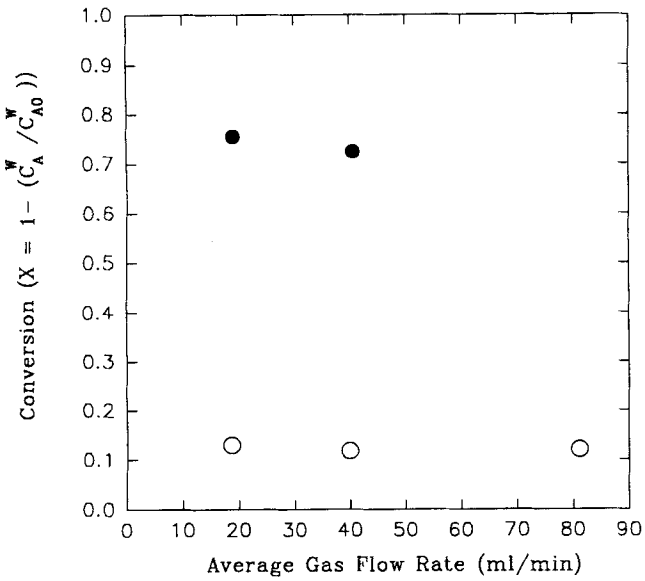

Figure 15. Degradation of phenol and toluene in membrane reactor 5: effects of ozonized oxygen flow rate variation on conversion, for FC43.

Phenol: ○ $C_{AO}^W = 147$ ppm; aqueous flow rate = 0.5 mL/min. **Toluene:** ● $C_{AO}^W = 70$ ppm; aqueous flow rate = 0.4 mL/min.

Figure 14 shows the highest conversion to be about 60% at an aqueous flow rate of 0.1 mL/min. As the aqueous flow rate is increased, it is obvious that the degradation of phenol moves away from a regime where the aqueous phase resistance is the controlling step to a regime where there is no specific controlling step. If a comparison is made between the performance of reactor 5 with that of the earlier polypropylene membrane-based reactors 1 to 4, it is clear that the earlier reactors (reactor 3, Figure 11 for phenol) did a much better job of degrading phenol at comparable aqueous flow rates. This can be attributed directly to the lower value of the surface area of the larger Teflon tubules in reactor 5 (5.1 cm^{-1} for reactor 5, as compared to 20.6–48.4 cm^{-1} for the polypropylene membrane-based reactors 1 to 4). Had a comparable surface area been available in reactor 5, the performance of the polypropylene membrane-based reactor would have been reproduced easily.

For pollutants having higher m_A into the organic phase, this behavior, though less prominent, is also clearly seen, for example, for toluene at aqueous flow rates of 0.1 mL/min the conversion is about 90%, compared with nearly 97% at aqueous flow rates of about 1.9 mL/min for the polypropylene membrane-based reactor 1 (Figure 13). For other compounds, namely, acrylonitrile, nitrobenzene and TCE, it is seen that high conversions are obtained at lower aqueous flow rates (about 85% for acrylonitrile at an aqueous flow rate of 0.1 mL/min, about 75% for nitrobenzene at an aqueous flow rate of 0.1 mL/min, and about 60% for TCE at an aqueous flow rate of 0.5 mL/min). From Figure 14, for acrylonitrile, nitrobenzene, toluene, and trichloroethylene, respectively, it is clear that the performance of the reactor is relatively independent of the inlet aqueous phase concentration. From Figure 14 it also becomes apparent that compounds with a higher m_A into the FC phase, like TCE and toluene, had comparatively higher removal rates for similar aqueous flow rates compared to compounds like phenol, acrylonitrile, and nitrobenzene.

The results shown in Figure 14 represent the operation of the same reactor 5 for each of the pollutants in turn *at steady state*. At low aqueous flow rates this involved operating the reactor for several hours to achieve steady state. During the experiments, especially when the reactor was operated at the low aqueous flow rates, the materials of construction, Teflon and silicone, were exposed to the harsh oxidizing environment of ozone and the other ongoing oxidation reactions for long hours (~ 6–8 h for each data point at the lowest flow rates). The reactor was exposed to ozone/ozonation reactions for a total period of 135 h (considering the five pollutants tested in turn) without any visible deterioration in reactor performance. This reflects the ruggedness of the membrane device with regards to its operation and durability. It is a drastic improvement over the previous membrane reactors made from polypropylene hollow fibers, namely, the materials of construction are stable. In addition this membrane reactor reduces drastically the evaporation of high-boiling FC phase, *if any*, into the gas phase.

Figure 15 shows the results of variation of gas flow rates on the reactor performance for phenol and toluene, covering the extremes of m_A into the FC phase. The results suggest that the gas phase resistance is not the controlling step and that the removal of the pollutant by stripping into the gas phase is virtually absent, at least in the present gas flow rate regime.

Conclusions

There is a great need for a compact add-on tubular reactor at the end of every waste stream containing hazardous organic compounds to detoxify such a stream economically at ambient temperature and pressure. The novel multiphase hollow fiber-based reactor of this study addresses such a need. This system requires a membrane reactor module, an ozonator with an air/O_2 supply, and a small FC reservoir; it suggests a modular, skid-mounted device that is small enough to be gainfully used at a remediation site or at the end of a waste stream containing hazardous organics. It has the ability to handle high organic strength wastewaters (feed inlet concentrations were about 120 ppm for toluene, 150 ppm for phenol, 150 ppm for acrylonitrile, 120 ppm for nitrobenzene, and 80 ppm for TCE). For most of these compounds (listed as priority pollutants by EPA) the conversions were in the range of 40 to 80%, depending upon the residence time and the type of pollutant being degraded. Two of these reactors in series could effectively handle a high strength wastewater.

The biphasic ozonation scheme has demonstrated higher ozonation efficiency compared to simple aqueous phase ozonation (since the FC phase has a much higher solubility for ozone than water). The problem of stability of the membrane materials in the reactor under the harsh oxidizing environment was resolved via the use of microporous Teflon tubules and silicone capillaries. The reactor ozonation efficiency can be drastically improved by using finer capillaries, resulting in increased surface area per unit volume for the reactor. The use of nonporous silicone capillaries hinders the stripping of any high boiling FC from the device, since these membranes do not allow direct contact between the stagnant FC phase and the gas phase, but at the same time are freely permeable to ozone. The FC phase used is a benign perfluorinated product and has found applications as a blood substitute; it has negligible solubility in water (< 7 ppm). The FC phase has virtually indefinite life, though further experiments would have to be conducted to verify such a supposition. The volume of FC phase required to fill the shell side is very little; the question of tainting it with organic compounds does not arise since it is a stationary phase and is constantly regenerated after ozone reacts with the pollutants and the oxidation products are removed by the mobile fluid phases.

Although a model based on the pseudo-first-order kinetics describes satisfactorily the degradation behavior of phenol in the membrane reactor, much more effort is needed to develop a model that describes the observed behavior vis-à-vis other pollutants. Second-order kinetics, axial variation on the ozone side, and ozone permeability through the wall of the gas supply fiber are aspects of importance in such a modeling effort. A question not yet answered is the nature of the degradation products; this would require extensive analytical research using gas chromatograph (GC) and mass spectrometry (MS). This will also provide a more accurate estimate of the stoichiometric ratio (b/a) and a more precise second-order rate constant. The formation of even more toxic by-products as a result of arcane reactions due to the presence of both protic and aprotic phases may not be a problem, for example, $COCl_2$, a product of oxidizing TCE in an aprotic environment, will immediately break down in the presence of water to CO_2 and HCl (Masten and Hoigné, 1992). Therefore it is quite likely that the presence of the two phases in intimate contact with one another may even hinder the formation of such compounds. Further experiments have to be carried out monitoring the Cl^- concentration in the aqueous phase for TCE as the model pollutant.

Acknowledgments

This research was conducted at Stevens Institute of Technology, Hoboken, NJ, and New Jersey Institute of Technology (NJIT), Newark, NJ, under two consecutive contracts from the Hazardous Substance Management Research Center (HSMRC) at NJIT, Newark, NJ. Studies based on reactor 5 were carried out at NJIT under a HSMRC contract to K. K. Sirkar and A. K. Guha. The authors would like to thank Anthony Green of IMPRA/IPE for the Teflon tubules and John Ruffing of 3M for the FC liquids.

Notation

C = concentration, mol/L
d_i = inner diameter of aqueous feed fiber, cm
d_o = outer diameter of aqueous feed fiber, cm
d_{lm} = logarithmic mean diameter of aqueous feed fiber, cm
D_A = diffusion coefficient of pollutant in organic phase, cm^2/s
k_2 = second-order reaction rate constant, s^{-1}
$\bar{k}$ = mass-transfer coefficient in the organic phase, defined by Eq. 32, cm/s
L = effective length of the module, cm
m_A, m_i = distribution coefficient of species A or i between organic and aqueous phase, Eq. 1
M_1 = defined by Eq. 13
M_2 = defined by Eq. 19
N_1 = defined by Eq. 14
N_2 = defined by Eq. 20
N_{Ay} = radial pollutant flux, $mol/cm^2 \cdot s$
N_{FT} = number of fibers on the wastewater side
Q_w = volumetric flow rate of the aqueous phase, mL/min
R_1 = defined by Eq. 15
R_2 = defined by Eq. 21
V = volume of liquid (for batch and semibatch model), mL
y = radial direction
X = conversion, defined by Eq. 40
z = axial direction
$\bar{}$ = organic phase (membrane reactor model)

Greek letters

δ_m = diffusion path from aqueous fiber OD to ozone fiber OD
ϵ = porosity of membrane
τ = tortuosity of membrane pore

Subscripts

$A0$ = pollutant at $t = 0$
Ai = pollutant at $y = 0$, as defined in Eq. 33
Ab = bulk aqueous phase
in = inlet of the reactor
out = outlet of the reactor

Literature Cited

Chen, S., H. Fan, and Y. K. Kao, "A Membrane Reactor with Two Dispersion Free Interfaces for Homogeneous Catalytic Reactions," *Chem. Eng. J.*, **49**, 35 (1992).

Froment, G. F., and K. B. Bischoff, *Chemical Reactor Analysis and Design*, Wiley, New York (1979).

Glaze, W. H., and J. W. Kang, "Advanced Oxidation Processes: Description of a Kinetic Model for the Oxidation of Hazardous Material in Aqueous Media with Ozone and Hydrogen Peroxide in a Semibatch Reactor," *Ind. Eng. Chem. Res.*, **28**, 1573 (1989).

Glaze, W. H., and J. W. Kang, "Advanced Oxidation Processes for Treating Groundwater Contaminated with TCE and PCE. Laboratory Studies," *J. AWWA*, **80**, 57 (1988).

Hoigné, J., and H. Bader, "Rate Constants of Reactions of Ozone with Organic and Inorganic Compounds in Water-I Non-Dissociating Organic Compounds," *Water Res.*, **17**, 173 (1983).
Itoh, N., and R. Govind, "Combined Oxidation and Dehydrogenation in a Palladium Membrane Reactor," *Ind. Eng. Chem. Res.*, **28**, 1554 (1989).
Joshi, M. G., and R. L. Shambaugh, "The Kinetics of Ozone-Phenol Reaction in Aqueous Solutions," *Water Res.*, **16**, 933 (1982).
Kim, J. S., and R. Datta, "Supported Liquid-Phase Catalytic Membrane Reactor-Separator for Homogeneous Catalysis," *AIChE J.*, **37**(11), 1657 (1991).
Langlais, B., D. A. Reckhow, and D. R., Brink, eds., *Ozone in Water Treatment, Application and Engineering*, Lewis, Ann Arbor, MI (1991).
Majumdar, S., A. K. Guha, and K. K. Sirkar, "A New Liquid Membrane Technique for Gas Separation," *AIChE J.*, **34**(7), 1135 (1988).
Majumdar, S., A. K. Guha, Y. T. Lee, and K. K. Sirkar, "A Two-Dimensional Analysis of Membrane Thickness in a Hollow-Fiber-Contained Liquid Membrane Permeator," *J. Memb. Sci.*, **43**, 259 (1989).
Masten, S. J., and J. Hoigné, "Comparison of Ozone and Hydroxyl Radical-Induced Oxidation of Chlorinated Hydrocarbons in Water," *Ozone Sci. Eng.*, **14**, 197 (1992).
Modell, M., G. G. Gaudet, M. Simson, G. T. Hong, and K. Biemann, "Supercritical Water Testing Reveals New Process Holds Promise," *Solid Wastes Manag.*, **25**, 26 (1982).
Nakagawa, T. W., L. J. Andrews, and R. M. Keefer, "The Kinetics of Ozonization of Polyalkybenzenes," *J. Chem. Soc.*, **82**, 269 (1960).
Perry, R. H., and D. W. Green, *Perry's Chemical Engineers' Handbook*, McGraw-Hill, New York, p. 3-286 (1984).
Prasad, R., and K. K. Sirkar, "Dispersion-Free Solvent Extraction with Microporous Hollow Fiber Modules," *AIChE J.*, **34**(2), 177 (1988).
Product Manual 3M Fluorinert Electric Liquids, 3M Industrial Chemicals Products Div., St. Paul, MN (1989).
Pryor, W. A., D. Giamalva, and D. F. Church, "Kinetics of Ozonation: 1. Electron Deficient Alkenes," *J. ACS*, **105**, 6858 (1983).
Pryor, W. A., D. Giamalva, and D. F. Church, "Kinetics of Ozonation: 2. Amino Acids and Model Compounds in Water and Comparisons to Rates in Nonpolar Solvents," *J. ACS*, **106**, 7094 (1984).
Shanbhag, P. V., "Kinetic Studies of Two-Phase Ozonation of Organic Pollutants in Wastewater," MS Thesis, Stevens Institute of Technology, Hoboken, NJ (1992).
Sirkar, K. K., "Other New Membrane Processes," *Membrane Handbook*, W. S. Winston Ho and K. K. Sirkar, eds., Van Nostrand Reinhold, New York (1992).
Skelland, A. H. P., *Diffusional Mass Transfer*, Wiley, New York, p. 162 (1974).
Stich, F. A., and D. B. Bhattacharyya, "Ozonolysis of Organic Compounds in a Two Phase Fluorocarbon-Water System," *Environ. Prog.*, **6**(4), 224 (1987).
Sundstrom, D. W., B. A. Weir, and H. E. Klei, "Destruction of Aromatic Pollutants by UV Light Catalyzed Oxidation with Hydrogen Peroxide," *Environ. Prog.*, **8**(1), 6 (1989).
Trivedi, D. H., "Destruction of Hazardous Organics in Wastewater Using a Novel Membrane Reactor," MS Thesis, Stevens Institute of Technology, Hoboken, NJ (1992).
Zimmerman, F. J., "New Waste Disposal Process," *Chem. Eng.*, **65**, 117 (1958).

Manuscript received May 2, 1994, and revision received Sept. 14, 1994.